

1 Remote sensing reveals fire-driven enhancement of a C₄ invasive alien 2 grass on a small Mediterranean volcanic island

3 Riccardo Guarino^{1*}, Daniele Cerra^{2*}, Renzo Zaia³, Alessandro Chiarucci⁴, Pietro Lo Cascio⁵, Duccio
4 Rocchini⁴, Piero Zannini⁴, Salvatore Pasta⁶

5 ¹Department of Biological, Chemical and Pharmaceutical Sciences and Technologies (STEBICEF), University of Palermo,
6 90123 Palermo, Italy

7 ²Remote Sensing Technology Institute (IMF), German Aerospace Center DLR, 82234 Oberpfaffenhofen, Germany

8 ³Magmatrek, 98050 Stromboli (ME), Italy

9 ⁴BIOME Lab, Department of Biological, Geological and Environmental Sciences, Alma Mater Studiorum, University of
10 Bologna, 40126 Bologna, Italy

11 ⁵NESOS, 98055 Lipari (ME), Italy

12 ⁶Institute of Biosciences and BioResources (IBBR), National Research Council, 90129 Palermo, Italy

13 *These authors contributed equally to this work.

14 **Correspondence:** Riccardo Guarino (riccardo.guarino@unipa.it)

15 **Abstract.** The severity and the extent of a large fire event that occurred on the small volcanic island of Stromboli (Aeolian
16 archipelago, Italy) on 25-26 May 2022 was evaluated through remotely sensed data to assess the short-term effect of fire on
17 local plant communities. For this purpose, the differential Normalised Burned Index (dNBR) was used also to quantify the
18 extent of early-stage vegetation recovery, dominated by *Saccharum biflorum* Forssk. (Poaceae), a rhizomatous C₄ perennial
19 grass of paleotropical origin. The burned area was estimated to have an extension of 337.83 ha, corresponding to 27.7% of the
20 island surface and to 49.8% of Stromboli's vegetated area. On the one hand, this event considerably damaged the native plant
21 communities, hosting many species of high biogeographic interest. On the other hand, *Saccharum biflorum* clearly benefited
22 from fire. In fact, this species showed a very high vegetative performance after burning, being able to exert unchallenged
23 dominance in the early stages of the post-fire succession. Our results confirm the complex and probably synergic impact of
24 different human disturbances (repeated fires, introduction of invasive alien plants) on the natural ecosystems of small volcanic
25 islands.

26 **Keywords.** Biological succession, Disturbance, Satellite imagery, Sprouters, Vegetation dynamics.

27 Introduction

28 Wildfires are a main disturbance factor affecting the Mediterranean terrestrial ecosystems, whose vegetation patterns are
29 largely influenced by interactions with fire. Fire frequency and severity delineates landscape attributes (Pausas, 2006; Jouffroy-
30 Bapicot et al., 2021), affects the structure and composition of the vegetation (Trabaud, 1994) and regulates speed and direction
31 of ecological succession dynamics (Canelles et al., 2019). Also, fire causes sudden variations in the carbon and energy balance
32 of ecosystems (Novara et al., 2013; Harris et al., 2016; Pausas & Millán, 2019) and in the soil microbial activity and functional
33 diversity of the microbiome (Velasco et al., 2009; Goberna et al., 2012).

34 At the onset of human civilisations, Mediterranean landscapes have been deeply modified by anthropogenic fires that were
35 used to expand the open-canopy space available for human activities and facilitate a wide array of foraging activities (Pausas
36 and Keeley, 2009). Throughout human history, demographic fluctuations, innovations and cultural exchanges have always
37 been accompanied by changes in land use and thus in fire regimes, amount and patchiness of fuel (Guyette et al., 2002; Driscoll
38 et al., 2021).

39 After the mid-20th century, land abandonment associated with an increase of woody cover and the build-up of fuels (Mantero
40 et al., 2020) chiefly contributed to the increased fire hazard in the Mediterranean Region (Le Houérou, 1993; Salis et al., 2022).
41 Despite the occurrence of some natural factors favouring fires, most of them are ignited by humans through carelessness or
42 voluntary action. Being the vegetation burning strongly related to plant water content (Bond and Wilgen, 1996), fires happen
43 mostly during the warmest and driest months, i.e. during the Mediterranean summer (Bergmeier et al., 2021). Climate change
44 scenarios indicate rising temperatures and decreasing amounts of precipitation, resulting in longer summer aridity, soil water
45 shortages and increasing fire risk (Moriendo et al., 2006; Lozano et al., 2017; IPCC, 2021), despite lower productivity may
46 limit fuel availability (Baudena et al. 2020).
47 Nevertheless, typical Mediterranean shrublands are highly resilient to relatively frequent, high-intensity fires, but changes in
48 the fire regime may make these communities susceptible to compositional changes, potentially followed by alien plant
49 invasions (Keely and Brennan, 2012; Vallejo et al., 2012). The positive feedback between invasive species and fire can be a
50 major cause of unidirectional change in invaded ecosystems (Brooks et al., 2004), and invasive species able to sustain an
51 increased fire frequency and intensity may generate favourable conditions for their self-perpetuation (Pauchard et al., 2008).
52 Small islands are particularly vulnerable to biological invasions (Bellard et al., 2016), due to the combined effect of the reduced
53 species pool and the competitive traits of invasive species. This process has been reported for Mediterranean islands (Celesti-
54 Grapow et al., 2016; Fois et al., 2020), particularly in the case of volcanic islands with ongoing or recent volcanic activity
55 (Karadimou et al., 2015; Pasta et al., 2017).
56 The Island of Stromboli (NE-Sicily) represents an ideal case-study for interaction between fires and invasive species, because
57 it has the lowest number of species, as expected by the within archipelago species-area relationship among the seven largest
58 islands of the Aeolian Archipelago (Chiarucci et al., 2021).
59 This study uses remotely sensed data to analyse the post-fire damage on local vegetation through the application of a spectrally
60 sensitive index, i.e. the differential Normalised Burned Index (dNBR), which has been used also to quantify the extent of the
61 subsequent early-stage vegetation recovery, dominated by *Saccharum biflorum*, in order to highlight the ecological behaviour
62 of this invasive alien species and its fire-driven ability to colonise new spaces.

63 **Material & Methods**

64 *Study area.* The Island of Stromboli, 12.6 km², represents the northeastern end of the Aeolian Archipelago, in southeastern
65 Tyrrhenian Sea, Mediterranean biogeographical region (Cervellini et al., 2020). Stromboli is the summit of the youngest and
66 most active of the Aeolian Islands; its subaerial activity began around 85 ka BP (Francalanci et al., 2013) and the emerged part
67 consists of a single cone that rises up to 926 m above sea level. The island has quite a regular slope averaging 28° and two
68 large horseshoe-shaped flank collapses named “Sciara del Fuoco”, on the northwestern-, and “Rina Grande”, on the
69 southeastern flank. Our study area covers an area of ca 3.4 km², between 50 m a.s.l. and 530 m a.s.l., on the northern and
70 eastern sides of Stromboli and can be roughly divided in two sectors. The northern sector is bounded by the “Fili del Fuoco”
71 ridge, overlooking “Sciara del Fuoco”, to the west and by the Vallonazzo valley to the east; the eastern sector is bounded by
72 the Vallonazzo valley to the north-west and by the “Rina Grande” depression to the south-east (Fig. 1). Both sectors are
73 characterised by medium to gentle slopes, with 80% of the area sloping less than 30° (Fornaciai et al., 2010).
74 The climate of Stromboli is typically Mediterranean. At 4 m a.s.l. the average yearly temperature is 18.2 °C, with a mean
75 temperature of 12.3 °C in the coldest (January) and 26 °C in the warmest month (August). The annual rainfall averages 570
76 mm, while the relative humidity is 75.0% in winter and 60.8% in summer. Based on the WorldClim interpolated maps (Hijmans
77 et al., 2005) and on the Rivas-Martínez bioclimatic classification (2004), the study area is characterised by an upper thermo-
78 mediterranean thermotype and a dry to sub-humid ombrotype (Bazan et al., 2015).
79 The study area was dominated by a typical Mediterranean rockrose garrigue (*Cistus creticus* subsp. *eriocephalus*, *C.*
80 *monspeliensis*, *C. salvifolius*) with scattered patches of maquis with *Genista tyrrhena*, *Spartium junceum*, *Olea europaea*,

81 *Erica arborea* and *Pistacia lentiscus* (Richter, 1984; Cavallaro et al., 2009). The former cultivated land and the volcanic ash
82 deposits were colonised by *Saccharum biflorum*, while small *Quercus ilex* stands were occasionally found along the impluvium
83 lines. Equally rare and scattered were the patches dominated by *Euphorbia dendroides*, limited to the rocky outcrops, especially
84 along the south-facing rim of Vallonazzo valley (Ferro and Furnari, 1968; Richter and Lingenhöhl, 2002). The highest and
85 southernmost end of the study area included part of the local population of *Cytisus aeolicus*, a narrow ranging endemic broom
86 growing only on the islands of Vulcano, Alicudi and Stromboli (Zaia et al., 2020).

87 On 25-26 May 2022, due to recklessness during the filming of a television drama, a fire broke out in the upper outskirts of the
88 village of San Vincenzo and, fuelled by a strong sirocco wind, burned the whole of our study area. While *Saccharum* stands
89 were entirely burned, a very few small patches of garrigue and *Quercus ilex* stands escaped from the fire.

91 *Target species.* By far the most common invasive alien species in Stromboli is *Saccharum biflorum* Forssk. [= *S. spontaneum*
92 L. subsp. *aegyptiacum* (Willd.) Hack.; henceforth: *Saccharum*], a vigorously growing rhizomatous grass of Palaeotropical
93 origin (Amalra and Balasundaram, 2006) with culms 1.5-2.5 m and flowering stems up to 3 m high. Its rhizomes can be up to
94 6 m long, with nodes every 10-15 cm, from which the culms and fascicled roots branch off (Supplement 1, Fig. S1). This
95 species has a C₄ metabolism and thrives in sandy-silty, often alluvial soils (Pignatti et al., 2017-2019).

96 As for the Aeolian Archipelago, *Saccharum* was introduced in the 19th century as a windbreak. Gussone (1832) recorded its
97 occurrence (despite wrongly identifying it as *Saccharum ravennae* L.) on the islands of Stromboli, Panarea, Lipari and
98 Vulcano, as “cultivated hedges in vineyards”. *Saccharum* has then spread on former cultivations, abandoned terraced fields
99 and wherever there was accumulation of volcanic ash, as noticed by Ferro and Furnari (1968, our translation): “a large part of
100 the north-eastern slope of the island, the very slope that Lojacono (1878) travelled through ‘vineyards that produce beautiful
101 wines’, is covered by dense, almost monophytic *Saccharum* vegetation, from sea level up to the upper limit of the ancient
102 crops (...). This slope could have been colonised in a different way by native floristic elements, but it is difficult to make
103 predictions on the final outcome of the competition, given the compactness of the *Saccharum* rhizomatous apparatus”.

104 However, photos published by Ferro and Furnari (1968) give the impression that 50 years ago *Saccharum* was more widespread
105 than nowadays. Besides cultivation abandonment, the establishment of this plant is favoured by fire, as observed by Richter
106 (1984). Local elder people recall a major spread of *Saccharum* soon after the fire caused by intense eruption in 1930 and the
107 subsequent abandonment of a large portion of the cultivated terraces along the eastern slopes of the island (Richter and
108 Lingenhöhl, 2002). Another large fire event, ignited at the Punta Labronzo landfill site in 1978, promoted the recovery of
109 *Saccharum* all over the eastern slopes above Punta Labronzo. In following years, the spread of this species has been somewhat
110 reduced by the development of native shrubland and garrigue, which until recently were the most widespread vegetation type
111 in the study area.

113 *Satellite imagery processing.* To infer the extent of fire damage to the vegetation and the post-fire surface of the resprouted
114 *Saccharum* patches, we used optical satellite images acquired by the spaceborne Sentinel-2 sensor, a multispectral mission
115 launched in the frame of the European Space Agency (ESA) Copernicus program (Drusch, 2012).

116 Sentinel-2 measures globally the backscattered solar radiation from ground targets with a temporal resolution of around 5 days,
117 across 13 spectral bands with different ground sampling distance (GSD) varying from 10 to 60 metres. In this work, we
118 employed the four bands at 10 m GSD, namely in the visible range (blue, green, red) and near infrared (NIR). Additionally,
119 we relied on Band 12 in the short-wave infrared (SWIR) at 20 m GSD to detect burned areas. Additionally, spectral bands 5,
120 6, 7, 8a, and 11, all at 20 m GSD, were used for the supervised classification of different vegetation types. All other bands at
121 60 m GSD were not used in this analysis. The products used were at processing level 2A, which provides radiometrically
122 corrected, georeferenced, orthorectified, atmospherically corrected, and converted to bottom of atmosphere reflectance data.
123 The choice of using reflectance rather than radiance products is motivated by the following reasons: (1) overall brightness

124 differences in different images due to different acquisition conditions are reduced in the level 2A products, (2) quantities
125 estimated from single images through spectral indices result more meaningful when applied to data in reflectance.
126 The data selection and processing were carried out on Google Earth Engine (GEE) (Amani et al., 2020), which is at the same
127 time a multi-petabyte repository of geo-referenced and harmonised Earth Observation raster, vector, and tabular datasets,
128 which includes the whole Sentinel-2 archive.

129 To quantify the damage caused by the above-mentioned fire event on the vegetation, different Sentinel-2 scenes acquired in a
130 relatively short time span were aggregated. An image composite of the island before the event was derived by considering 8
131 acquisition dates with cloud cover below 5% acquired before the fire event, from April 15 to May 22, 2022, and considering
132 the median reflectance for each image element. This allows removing abnormal values due to specific atmospheric conditions
133 inducing error in the reflectance estimation process, undetected clouds, and cloud shadows in the scene. The post-fire
134 reflectance was estimated by applying the same processing to 6 acquisition dates after the event, from May 26 to June 15,
135 2022. The two image composites are reported in Fig. 2. Therein, pre- and post-event true colour images obtained from Sentinel-
136 2 bands in the visible range (namely bands 4, 3, and 2) can be visually assessed, with damage caused by the fire in the
137 northeastern part of the island already evident in this band combination.

138 In order to estimate vegetation loss and total burned area, we derived the Normalised Burn Ratio (*NBR*), defined for a
139 multispectral image x as:

$$140 \quad NBR(x) = \frac{NIR - SWIR}{NIR + SWIR}$$

141 where *NIR* and *SWIR* indicate reflectance in the Near and Short-wave Infrared, represented for Sentinel-2 by the bands 8 and
142 12, respectively. The *NBR* is a commonly used index to detect burned area and burn severity (Key and Benson, 1996), and is
143 particularly sensitive to the changes in the amount of live green vegetation, moisture content, and some soil conditions which
144 may occur after fire (Lentile et al., 2006).

145 Change detection relying on spectral indices from multitemporal pre- and post-fire images can be used to estimate vegetation
146 loss or recovery. Relying on the availability of multitemporal images, we used the differenced *NBR* (*dNBR*) since it performs
147 well in capturing the spatial severity within fire perimeters (Picotte and Robertson, 2010; Soverel et al., 2010).

148 The *dNBR* related to pre- and post-event images, respectively x_{t_0} acquired at time t_0 and x_{t_1} acquired at time t_1 , is the delta
149 of the two measurements:

$$150 \quad dNBR(x_{t_0}, x_{t_1}) = NBR(x_{t_0}) - NBR(x_{t_1})$$

151 This quantity has been used to estimate both fire severity and vegetation recovery after the fire event: a negative *dNBR* is
152 correlated to recovery after fires, while a positive one indicates damages, with severity proportional to the *dNBR* value.

153 We first estimated the area affected by fire immediately after the event by computing the *dNBR* for the whole island. The
154 affected area was derived by applying the damage classes defined in (Key and Benson, 1996). In particular, the value of *dNBR*
155 in the middle of the range related to low-severity damage (0.1-0.27) and approximated to the second decimal digit, in the
156 specific 0.19, was selected and assessed using expert knowledge in order to exclude false positives from the estimation and
157 perform further analysis only on relevant image elements, considering damaged all image elements with *dNBR* above this
158 threshold (Fig. 2). This was necessary as using the value of 0.1 was raising false alarms, most notably within urban areas.

159 To check whether the severity of the damage was related to geomorphological features, rather than to different vegetation
160 units, the correlation between results of the *dNBR* and a digital elevation model (DEM), was evaluated. The Normalized
161 Difference Vegetation Index (*NDVI*; Gandhi et al., 2015) was also applied to estimate the loss in live green vegetation, and its
162 correlation with *dNBR* values was checked (Supplement 2).

163 Finally, to evaluate the quality of our results, we computed a new *dNBR* between the pre-event image and a mosaic of Sentinel-
164 2 acquisitions from the time range 15-17 August 2022. The burned area detected in such way was compared with very high-
165 resolution images acquired by a drone DJI Phantom 3 professional on 17 August 2022, i.e. around 3 months after the fire event
166 and 5 days after the first intense rainstorm. Drone images were merged and geo-referenced through the software Agisoft

167 Photoscan Professional (version 1.2.6). These images have 10 cm GSD and have been mosaicked over the north-eastern part
168 of the island, covering the inhabited area of San Bartolo and San Vincenzo. The drone images did not cover the higher
169 elevations of our study area, closer to the volcano's vents, nor the northernmost part, near Punta Labronzo (Fig. 4).
170

171 *Vegetation recovery assessment.* The mentioned image composite of Stromboli derived from 8 acquisitions from April-May
172 2022 was also used to map the structural types of the vegetation affected by the fire, through supervised classification based
173 on spectral information. Three vegetation classes have been defined: maquis, garrigue, and Saccharum. The class "maquis"
174 groups tall woody vegetation patches, namely: (1) shrublands with *Genista tyrrhena*, *Spartium junceum*, *Erica arborea* and
175 *Pistacia lentiscus*, (2) abandoned olive groves invaded by *Cytisus infestus* and *C. laniger*, (3) *Quercus ilex* groves, (4)
176 *Euphorbia dendroides* shrublands, and (5) *Cytisus aeolicus* shrublands. The class "garrigue" refers to vegetation patches with
177 dwarf shrubs, subshrubs and bunchgrasses, including (1) dwarf shrublands dominated by *Cistus sp. pl.*, (2) herbaceous-
178 chamaephytic vegetation dominated by *Cymbopogon hirtus*, *Oloptum miliaceum*, *Centranthus ruber*, *Jacobaea maritima*
179 subsp. *bicolor* and *Scrophularia canina*, (3) small impluvia colonized *Rubus sp.* and *Pteridium aquilinum*. Finally, the
180 vegetation patches dominated by *Saccharum* were attributed to the class "Saccharum", easily recognized by its typical
181 yellowish-green colour and remarkable structural homogeneity, given by one single species covering well over 80% of the
182 soil. These patches have two different textures: smoother where *Saccharum* has invaded abandoned vineyards, more granular
183 where *Saccharum* has invaded former fig tree plantations, as it happened in the upper part of our study area.

184 For each of the three classes described above, 10 patches of 50 pixels each were selected by experts to constitute the training
185 dataset and 150 random points equally split among the three classes constituted the validation dataset. The area where damage
186 occurred was fed to a Support Vector Machine (SVM) classifier (M.A. Hearst et al., 1998), as implemented in the *libsvm*
187 routine in GEE, using a linear kernel and setting the cost *C* to 1. The input parameters were all Sentinel-2 spectral bands having
188 a Ground Sampling Distance of 10 or 20 meters, namely bands 2 to 8, 8a, 11, and 12. The results of the classification algorithm
189 (Fig. 3) were evaluated through visual analysis by the experts and numerically validated using the validation dataset, yielding
190 an overall accuracy higher than 90%.

191 To check variations in the distribution of burn severity levels and to evaluate the short-term response after fire among different
192 vegetation types, the pixel values of *dNBR* pre-post were randomly sampled in 50 random points for each of the three
193 vegetation classes described above. Levene's test was used to assess the homogeneity of variance, followed by nonparametric
194 Kruskal-Wallis test, using Chi-Square distribution (right-tailed) and Dunn's post hoc comparison to reject the null hypothesis.

195 To evaluate the short-term vegetation response after fire, the composite images of Sentinel-2 acquisitions from the following
196 time ranges were analyzed: 15-17 August 2022; 14-26 September 2022; 22-28 October 2022; 10 May-15 June 2023.

197 On-site surveys were carried out on 15-19 September 2022, 7-9 March and 9-12 September 2023, to validate the remotely
198 sensed data and to sample vegetation plots in the burned area. The vegetation was sampled in 38 plots, 10 m² each, randomly
199 selected along a belt between 180 and 220 m elevation (Fig. 1). To optimize the sampling effort, the location of the sampling
200 sites deviated little from the paths that run along the volcano's flank above the villages of St. Vincent and St. Bartolo. The only
201 rules adopted were that the plots should have been at least 50 m apart, to avoid spatial autocorrelation, and that each of the
202 above-mentioned three vegetation classes should have been represented by at least 10 plots. Vegetation data were collected
203 using a modified Braun-Blanquet (1964) approach, by visually estimating the cover-abundance in percentage values and by
204 measuring the mean and maximum height (in cm) of each species.

205 To collect useful information to better understand the interaction between *Saccharum* and fire, a comparative evaluation of
206 stem density/m² in burned vs. unburned patches, was carried out in the field on 18 September 2002. Sampling plots 1 × 1 m
207 were located every 100 m along two almost contiguous transects, 900 m long, ten inside the burned area, above the village of
208 San Vincenzo and 10 outside the burned area, in the bottom part of Rina Grande (Fig. 1). In each plot, the number of stems of
209 *Saccharum* was counted and the average and max. height were recorded. In the unburned patches, the relative percentage of

210 dry stems compared to green stems was also assessed, to showcase the ease of fire ignition due to the abundant presence of
211 dry biomass, consisting mainly of the flowering stems of *Saccharum* which, once faded, dry out completely but remain
212 standing, as they are supported by the green stems which have not yet flowered.
213

214 **Results**

215 The application of the *dNBR* yielded a severity map showing the difference between pre- and post-fire acquisitions. The burned
216 area was quantified in 337.83 ha, corresponding to 27.7% of the island surface (Fig. 2). Concerning the burn severity (Keeley
217 2009), 75.15 ha showed low, 218.37 ha intermediate and 44.31 ha high severity level. The Kruskal-Wallis H test indicated a
218 significant difference in the distribution of severity levels among vegetation classes, $\chi^2(2) = 8.56$, $p = .013$, having the burned
219 garrigue and maquis suffered higher severity damage than *Saccharum* (Fig. 3).

220 We found no correlation between the *dNBR* and neither the elevation nor the slope (therefore not reported here). *NDVI* values
221 were strongly correlated with *dNBR* values (Pearson correlation of 0.97, see Supplement 2). However, *NDVI* showed some
222 noise in the estimation of vegetation loss, and false positives scattered across the inhabited area. Therefore, these results are
223 not reported further in this paper, despite of *NDVI* having a true resolution of 10 m in Sentinel-2 products, while *NBR* employs
224 the SWIR band, which is originally at 20 m GSD and therefore interpolated.

225 Considering the limitations imposed on spatial resolution by the satellite-derived damage evaluation, the burned area detected
226 by *dNBR* from the mosaic of Sentinel-2 acquisitions in the time range 15-17 August 2022 matched well the burned area
227 observable in the drone image acquired on August 17th, with human-made structures and even single trees that were spared
228 by the fire correctly regarded as undamaged in the *dNBR* estimation (Fig. 4). At the same time, partially burned vegetated
229 areas were correctly included in *dNBR* results, because even if they did not burn completely a steep decrease in the red edge
230 portion of the spectrum around 700 nm revealed strong vegetative stress.

231 The *NDVI* calculated with a threshold of 0.08, therefore quantifying all pixels having at least 8% covered by photosynthetically
232 active vegetation, quantified the area of the island covered by vegetation before the fire as 678.73 ha. Considering the described
233 correlation between *dNBR* and *NDVI*, and the area affected by the fire as computed by *dNBR*, it can be concluded that roughly
234 half (49.8%) of the vegetated area of Stromboli has been burned during the fire event.

235 Figure 5 shows the vegetation recovery in the area affected by the fire. According to the thresholds suggested by Key and
236 Benson (1996) to categorise recovery levels from *dNBR* values, in the specific enhanced low and high regrowth for *dNBR*
237 values ranging from -100 to -250 and smaller than -250, respectively, one year after fire 53.25% of the burned area showed
238 high enhanced recovery, 30.84% low recovery, 15.9% no recovery. Among the three vegetation classes considered, 56.08%
239 of the pixels with high recovery levels were *Saccharum*, 38.2% garrigue and 5.7% maquis. Conversely, 10.46% of the areas
240 with no recovery were maquis, 65.48% garrigue and 23.856% *Saccharum*. Considering the distribution of recovery levels
241 across the first growing season after fire, *Saccharum* is clearly characterized by faster recovery with respect to the maquis and
242 the garrigue, particularly at the beginning of the first growing season after fire (September-October 2022).

243 Referring to the vegetation recovery estimated in October 2022, the Kruskal-Wallis H test indicated that there is a significant
244 difference among the vegetation classes, $\chi^2(2) = 8.41$, $p = .015$, with a mean rank score of 64.06 for *Saccharum*, 89 for garrigue,
245 and 73.44 for maquis. The Post-Hoc Dunn's test using a Bonferroni corrected alpha of 0.017 indicated significant differences
246 of *Saccharum* recovery towards both maquis and garrigue (Table 1).
247

248 **Table 1. Dunn's post hoc comparison for *dNBR*-estimated recovery of the considered vegetation classes in the burned**
249 **area on October 2022.**

Pair	Mean Rank difference	Z	SE	p-value	p-value/2
<i>Saccharum</i> -maquis	-24.94	2.8703	8.6891	0.004101	0.002051
<i>Saccharum</i> -garrigue	15.56	1.7908	8.6891	0.07333	0.03667
garrigue-maquis	-9.38	1.0795	8.6891	0.2804	0.1402

250

251

252

253

254

255

256

257

258

259

260

261

The results of the spectral evaluation of the vegetation recovery are confirmed by the on-site surveys. Table 2 shows the median values of percentage cover and height of resprouts and seedlings in the plots sampled on September 2022, March and September 2023. The distribution of the plots across the vegetation classes was the following: 10 *Saccharum*, 16 Garrigue, 12 Maquis. The Kruskal-Wallis H test indicated highly significant differences ($p < 0.001$) between the cover values and height of resprouts and cover of seedlings in the *Saccharum* plots compared to those ascribed to the other two vegetation classes. No significant difference was found in seedlings height or even in species composition across the vegetation classes (data not shown), which in all cases was largely dominated by annual plants such as *Brassica fruticulosa*, *Ornithopus compressus*, *Lupinus angustifolius*, *Trifolium stellatum* and by seedlings of *Cistus* sp.pl. (mainly *Cistus creticus*).

Table 2. Median values of cover (%) and height (cm) of resprouts and seedlings in the validation plots. Values in brackets indicate positive absolute deviations from the median values.

Date	Vegetation	Resprouts cover	Resprouts height	Seedlings cover	Seedlings height
15-19 Sept. 2022	<i>Saccharum</i>	85 (5)	150 (20)	5 (0)	9 (13)
	Garrigue	10 (15)	8 (17)	25 (25)	13 (21)
	Maquis	15 (15)	15 (12)	30 (30)	14 (16)
7-9 March 2023	<i>Saccharum</i>	90 (0)	160 (20)	10 (5)	43 (14)
	Garrigue	20 (10)	23 (24)	40 (20)	33 (22)
	Maquis	20 (15)	27 (38)	50 (25)	38 (25)
9-12 Sept. 2023	<i>Saccharum</i>	90 (0)	160 (20)	10 (10)	53 (19)
	Garrigue	25 (15)	20 (32)	55 (15)	47 (32)
	Maquis	25 (30)	36 (47)	50 (20)	55 (30)

262

263

264

265

266

The estimated vegetation composition in the study area shows that already in August resprouting *Saccharum* had invaded approximately 13% of areas previously occupied by other vegetation classes, especially along gullies. This latter percentage remained almost unchanged in the following months (Fig. 6). The fast recovery of the *Saccharum* patches, with their soft green colour standing out against the surrounding black, became evident as early as a few weeks after the fire (Supplement 1, Fig.

267 S3-5). Until first rains, which occurred on the night of 12 August 2022, *Saccharum* was the only green spot in the fire-affected
268 areas and the high-resolution drone images captured on 17 August 2022 clearly show all *Saccharum* patches in their recovery
269 phase (Fig. 4). In the Sentinel2 images of September-October 2022, previous damage from the fire event appears mitigated.
270 More in detail, a total of 110 ha of the previously burned area (roughly one third) exhibits a *dNBR* value below -0.1, which
271 represents a strong indicator of vegetation recovery. This was mostly due to *Saccharum*, demonstrating that this species can
272 exert unchallenged dominance in the early stages of the post-fire dynamics (succession), reaching vegetative stem densities
273 only slightly lower than those of the unburned stands in a short time (Fig. 7).

274 Discussion

275 Our study confirms that fire severity can be mapped with high accuracy using indices derived from Sentinel 2 imagery with
276 supervised vegetation classification based on spectral information (Gibson et al. 2020). Fire is a major driving force for
277 Mediterranean insular ecosystem dynamics since the emergence of the Mediterranean climate (Médail, 2021), particularly in
278 volcanic island ecosystems (Irl et al., 2014). This paper provides the first report of how a single fire event significantly affected
279 Stromboli Island, burning 50% of the vegetated island surface. This clearly influenced the island biota, particularly the native
280 vegetation, which is rich in species of relevant biogeographic interest, such as *Centaurea aeolica*, *Genista tyrrhena*, *Dianthus*
281 *rupicola* subsp. *aeolicus*, *Jacobaea maritima* subsp. *bicolor* (Pasta et al., submitted). In addition, the highest and southernmost
282 end of the study area included part of the *Cytisus aeolicus* population, one of the rarest and most emblematic endemic plant
283 species of the Aeolian Archipelago (Zaia et al., 2020).

284 Although we applied a permissive threshold (8%) in the NDVI for our quantitative analysis, our conclusion that the fire
285 occurred on 25-26 May 2022 burned roughly half of Stromboli's vegetated area appears reasonably accurate, when considering
286 all the available data we used for validation. Our study confirms that burn severity levels, estimated by *dNBR*, is higher in
287 woody vegetation (Koutsias & Karteris, 2002), presumably due to the larger above-ground biomass and dead organic matter
288 stock in the case of maquis (Rossetti et al. 2022) and to the high flammability of Mediterranean dwarf shrubs in the case of
289 garrigue (Dimitrakopoulos, 2001). Despite the garrigue being mostly formed by pyrophytes, obligate seeders, and among the
290 first shrubs to emerge after fire (Palá-Paúl, 2005; Athanasiou et al., 2023), our study demonstrated that *Saccharum* exhibits
291 even greater resilience compared to garrigue in the earliest stages after fire, with a clear risk of altering the recovery patterns
292 of native vegetation, that especially on volcanic islands are characterized by high abundance of nitrogen fixers and annual
293 species (Weiser et al., 2021).

294 The positive interaction between *Saccharum* and fire was already noticed in Stromboli by Richter (1984) and Richter and
295 Lingenhöhl (2002). Fire spreads very easily across *Saccharum* vegetation, due to the abundant presence of standing dry
296 biomass (Supplement 1, Fig. S2, S4, S6). This result agrees with many recent studies focused on the role of fire as promoter
297 of C₄ grasses (Scheiter et al., 2012; Hoetzel et al., 2013; Ripley et al., 2015). Although the native rockrose garrigue vegetation
298 is also adapted to - and favoured by - periodical fires (Pausas, 1999), its survival derives from the ability of *Cistus* to develop
299 a long-lasting soil seed bank (Soy and Sonie, 1992; Scuderi et al., 2010). Too frequent fire events and runoff caused by heavy
300 rainfall on sandy and incoherent soils may cause a critical depletion of soil seed bank and favour sprouters against obligate
301 seeders. On this purpose, we must point out that the autochthonous sprouters (such as *Erica arborea*, *Pistacia lentiscus*, *Olea*
302 *europaea*) have slower growth rate than *Saccharum* and need longer time to become established.

303 After the fire, our study area was exposed to full solar radiation; dark sandy surfaces were subject to extreme microclimatic
304 (surface temperatures up to 80 °C; see Richter, 1984) and extremely dry conditions. These were not favourable for the
305 germination of the soil seed bank, whilst sprouters faced almost no competition until first rains, which occurred on 12 August
306 2022. The first and most important beneficiary of these contrasting conditions was *Saccharum*, which over time was able to
307 colonise large surfaces of tephra in the northern and eastern parts of the island, likely due to a positive interaction between
308 land abandonment, repeated fires and volcanic ash deposition. *Saccharum* is extremely competitive thanks to a variety of

309 functional strategies (e.g. C₄ photosynthetic pathway, large resource allocation belowground, into clonal and bud-bearing
310 rhizomes which can boost a quick resprouting and local spread/space occupancy/resource uptake) under current and probably
311 also under predicted conditions (likely more disturbed) which could affect and define different ecosystems on Stromboli.
312 According to Lojacono (1878), *Saccharum* was planted along the vineyards to shelter them from the northerly winds (Fig. 8).
313 This condition lasted until the eruption of 11 September 1930, so far considered the most violent and destructive event in the
314 historical records of Stromboli's activity (Rittmann, 1931). Facilitated by the winter rains and by a rapid expansion via
315 rhizomes, *Saccharum* first benefited from the emigration of most inhabitants and subsequent abandonment of terraced fields,
316 which in a very short time lapse were almost completely sealed off by a dense monospecific bed, which made it difficult for
317 other species to establish themselves (Ferro and Furnari, 1968; Richter, 1984). Since then, competition for space between local
318 native vegetation and *Saccharum* beds has been regulated mainly by the periodical occurrence of fires. Further studies are
319 needed to understand the duration of the *Saccharum* expansion phases. Our preliminary results suggest that the expansion of
320 *Saccharum* is surprisingly fast, but the decline may also be relatively rapid. There is no data on the longevity of *Saccharum*
321 rhizomes and related senescence processes, nor on the effects of volcanic ash deposition on rhizome burial. However, there
322 are reasonable indications that, if the vegetation is not too frequently affected by fire, *Saccharum* could be gradually replaced
323 by native vegetation within a few decades, as captured in the maps published as "Fig. 4" by Richter and Lingenhöhl (2002).
324 On 12 August 2022, a severe thunderstorm triggered disastrous erosion processes over the entire area affected by the fire on
325 May 25-26. Large quantities of mud, stones and volcanic ashes flooded the streets of the villages San Bartolo and San Vincenzo
326 (Supplement 1, Fig. S7). In the burned area, the traces of runoff and surface rill erosion were still very evident during our
327 inspections on 18-19 September 2022. However, just as evident was the ambivalent role of *Saccharum*, which, while on the
328 one hand clearly prevails on native species, on the other hand, thanks to its dense mat of rhizomes, proves to be much more
329 efficient than the burned native vegetation in counteracting hydrogeological instability. The latter is a very relevant aspect in
330 a volcanic island, whose soils are largely made up of loose tephra ashes.

331 Over time, *Saccharum* beds have become an important secondary habitat for many animal species. In fact, they represent the
332 main breeding site for at least 70% of breeding bird species on Stromboli (Massa et al., 2015) and host conspicuous populations
333 of almost all terrestrial vertebrates occurring on the island (especially *Tarentola mauritanica*, *Podarcis siculus* and *Hierophis*
334 *viridiflavus*). Some of the invertebrates that occurs in the *Saccharum* beds are of considerable biogeographic interest, such as
335 *Caulostrophus zancleanus*, a regional endemic (Lo Cascio et al., 2022), and the recently described *Catomus aeolicus*, endemic
336 of the northeastern sector of the Aeolian archipelago (Ponel et al., 2020). Although not specialised on *Saccharum*, the
337 rhizophagous larvae of the melolonthid *Anoxia orientalis*, a species considered rare at national scale in Italy, feed on its
338 rhizomes. Surprisingly enough, *S. biflorum* does not seem to be an attractive fodder for the mammals introduced in historical
339 (*Oryctolagus cuniculus*) or more recent (*Capra hircus*) times, nor significant infestations of phytophagous insects have ever
340 been observed. Thus, herbivory does not seem to be a limiting factor to the expansion of *Saccharum* on Stromboli.

341 **Conclusions**

342 Remotely sensed data provide fast, accurate and reliable information for post-fire damage analysis, being spectrally sensitive
343 to vegetation features and structure. Multi-temporal data acquisition allows observations on early-stage vegetation dynamics
344 which, in our case, point out the outstanding pioneer role played by *Saccharum biflorum*, showcasing its ability to colonize
345 and dominate large areas, potentially altering the recovery patterns of native vegetation. On the other hand, *Saccharum* proves
346 to be efficient in stabilizing the soil, especially in a volcanic island with loose tephra ashes, thus mitigating the erosion
347 processes. Our findings underscore the complex interplay between fire, vegetation dynamics, and ecosystem recovery on
348 Stromboli, emphasizing the need for further research to better understand the long-term dynamics of *Saccharum* expansion
349 and its interactions with native biota.

350

351 *Author contribution.* RG and DC developed the research idea, DC processed satellite and drone imagery, RG and RZ conducted
352 the field work, RG led the writing process, all authors discussed the results and contributed to the manuscript.

353

354 *Acknowledgements.* We would like to thank Giuseppe De Rosa, who brought DC and RG together, and Antonio Zimbone for
355 driving the drone flight and taking the pictures used to check the quality of the information derived from dNBR analysis. Three
356 anonymous reviewers and Gianluigi Ottaviani are gratefully acknowledged for their suggestions on an earlier version of the
357 manuscript.

358

359 *Competing interests.* The contact authors declared that neither they nor their co-authors have any competing interests.

360 **References**

361 Amalraj, V. A., and Balasundaram, N.: On the taxonomy of the members of ‘*Saccharum* complex’. *Genetic Resources and*
362 *Crop Evolution*, 53, 35–41, <https://doi.org/10.1007/s10722-004-0581-1>, 2006.

363 Amani, M., Ghorbanian, A., Ahmadi, S. A., Kakooei, M., Moghimi, A., Mirmazloumi, S. M., Moghaddam, S. A. H., Mahdavi,
364 S., Ghahremanloo, M., Parsian, S., Wu, Q., and Brisco, B.: Google earth engine cloud computing platform for remote sensing
365 big data applications: A comprehensive review. *IEEE Journal of Selected Topics in Applied Earth Observations and Remote*
366 *Sensing*, 13, 5326–5350, <https://doi.org/10.1109/JSTARS.2020.3021052>, 2020.

367 Athanasiou, M., Martinis, A., Korakaki, E., and Avramidou, E. V.: . Development of a Fuel Model for *Cistus* spp. and Testing
368 Its Fire Behavior Prediction Performance. *Fire* 2023, 6, 247, <https://doi.org/10.3390/fire6070247>, 2023.

369 Baudena, M., Santana, V.M., Baeza, M.J., Bautista, S., Eppinga, M.B., Hemerik, L., Garcia Mayor, A., Rodriguez, F.,
370 Valdecantos, A., Vallejo, V.R., Vasques, A., and Rietkerk, M.: Increased aridity drives post-fire recovery of Mediterranean
371 forests towards open shrublands. *New Phytologist*, 225(4), 1500-1515, <https://doi.org/10.1111/nph.16252>, 2020.

372 Bazan, G., Marino, P., Guarino, R., Domina, G., and Schicchi, R.: Bioclimatology and vegetation series in Sicily: A
373 geostatistical approach, *Annales Botanici Fennici*, 52, 1–18, <https://doi.org/10.5735/085.052.0202>, 2015.

374 Bergmeier, E., Capelo, J., Di Pietro, R., Guarino, R., Kavgacı, A., Loidi, J., Tsiripidis, J., and Xystrakis, F.: ‘Back to the
375 Future’—Oak wood-pasture for wildfire prevention in the Mediterranean, *Plant Sociology*, 58, 41–48,
376 <https://doi.org/10.3897/pls2021582/04>, 2021.

377 Bellard, C., Cassey, P., and Blackburn, T. M.: Alien species as a driver of recent extinctions, *Biology Letters* 12, 20150623,
378 <https://doi.org/10.1098/rsbl.2015.0623>, 2016.

379 Bond, W. J., and Wilgen, B. W.: Why and how do ecosystems burn?, *Fire and plants: Population and Community Biology*
380 *Series 14*: 16–33. Springer, Dordrecht, 1996.

381 Brooks, M.L., D’Antonio, C.M., Richardson, D.M., Di Tomaso, J.M., Grace, J.B., Hobbs, R.J., Keeley, J.E., Pellant, M., Pyke,
382 D.: Effects of invasive alien plants on fire regimes. *Bioscience*, 54, 677–688, [https://doi.org/10.1641/0006-3568\(2004\)054\[0677:EOIAPO\]2.0.CO;2](https://doi.org/10.1641/0006-3568(2004)054[0677:EOIAPO]2.0.CO;2), 2004.

384 Canelles, Q., Aquilué, N., Duane, A., and Brotons, L.: From stand to landscape: modelling post-fire regeneration and species
385 growth, *Ecological Modelling*, 404, 103–111, <https://doi.org/10.1016/j.ecolmodel.2019.05.001>, 2019.

386 Cavallaro, F., Morabito, M., Navarra, E., Pasta, S., Lo Cascio, P., Campanella, P., Cavallaro, M., Cavallaro, A., Merenda, A.,
387 Di Procolo, G., Rühl, J. and Ioppolo, G.: Piano di Gestione dei Siti Natura 2000 delle Isole Eolie. Regione Siciliana,
388 Assessorato Territorio e Ambiente, 2009.

389 Celesti-Grapow, L., Bassi, L., Brundu, G., Camarda, I., Carli, E., D’Auria, G., Del Guacchio, E., Domina, G. Ferretti, G.,
390 Foggi, B., Lazzaro, L., Mazzola, P., Peccenini, S., Pretto, F., Stinca, A., and Blasi, C.: Plant invasions on small Mediterranean
391 islands: An overview, *Plant Biosystems*, 150(5), 1119–1133, <https://doi.org/10.1080/11263504.2016.1218974>, 2016.

392 Cervellini, M., Zannini, P., Di Musciano, M., Fattorini, S., Jiménez-Alfaro, B., Rocchini, D., Field, R., Vetaas O.R., Irl, S.D.H.,
393 Beierkuhnlein, C., Hoffmann, S., Fischer, J.-C., Casella, L., Angelini, P., Genovesi, P., Nascimbene, J. and Chiarucci, A.: A
394 grid-based map for the Biogeographical Regions of Europe. *Biodiversity Data Journal*, 8, e53720,
395 <https://doi.org/10.3897/BDJ.8.e53720>, 2020.

396 Chiarucci, A., Guarino, R., Pasta, S., La Rosa, A., Lo Cascio, P., Médail, F., Pavon, D., Fernández-Palacios, J. M., and Zannini,
397 P.: Species-area relationship and small-island effect of vascular plant diversity in a young volcanic archipelago, *Journal of*
398 *Biogeography*, 48(11), 2919–2931, <https://doi.org/10.1111/jbi.14253>, 2021.

399 Dimitrakopoulos, A.P.: A statistical classification of Mediterranean species based on their flammability components.
400 *International Journal of Wildland Fire*, 10, 113–118, <https://doi.org/10.1071/WF01004>, 2001.

401 Driscoll, D. A., Armenteras, D., Bennett, A. F., Brotons, L., Clarke, M. F., Doherty, T.S., Haslem, A., Kelly, L.T., Sato, C.F.,
402 Sitters, H., Aquilué, N., Bell, K., Chadid, M., Duane, A., Meza-Elizalde, M.C., Giljohann, K.M., González, T.M., Jambhekar,
403 R., Lazzari, J., Morán-Ordóñez, A. and Wevill, T.: How fire interacts with habitat loss and fragmentation, *Biological*
404 *Reviews*, 96(3), 976–998, <https://doi.org/10.1111/brv.12687>, 2021.

405 Drusch, M., Del Bello, U., Carlier, S., Colin, O., Fernandez, V., Gascon, F., Hoersch, B., Isola, C., Laberinti, P., Martimort,
406 P., Meygret, A., Spoto, F., Sy, O., Marchese, F., and Bargellini, P. : Sentinel-2: ESA's optical high-resolution mission for
407 GMES operational services, *Remote Sensing of Environment*, 120, 25–36, <https://doi.org/10.1016/j.rse.2011.11.026>, 2012.

408 Ferro, G. and Furnari, F.: Flora e vegetazione di Stromboli (Isole Eolie), *Archivio Botanico e Biografico Italiano*, 44(1–2),
409 21–45, 1968.

410 Fois, M., Podda, L., Médail, F., and Bacchetta, G.: Endemic and alien vascular plant diversity in the small Mediterranean
411 islands of Sardinia: Drivers and implications for their conservation, *Biological Conservation*, 244, 108519,
412 <https://doi.org/10.1016/j.biocon.2020.108519>, 2020.

413 Fornaciai, A., Bisson, M., Landi, P., Mazzarini, F., and Pareschi, M. T.: A LiDAR survey of Stromboli volcano (Italy): Digital
414 elevation model-based geomorphology and intensity analysis, *International Journal of Remote Sensing*, 31(12), 3177–3194,
415 <https://doi.org/10.1080/01431160903154416>, 2010.

416 Gibson, R., Danaher, T., Hehir, W., and Collins, L.: A remote sensing approach to mapping fire severity in south-eastern
417 Australia using sentinel 2 and random forest. *Remote Sensing of Environment*, 240, 111702,
418 <https://doi.org/10.1016/j.rse.2020.111702>, 2020.

419 Goberna, M., García, C., Insam, H., Hernández, M. T., and Verdú, M.: Burning fire-prone Mediterranean shrublands:
420 immediate changes in soil microbial community structure and ecosystem functions, *Microbial Ecology*, 64(1), 242–255,
421 <https://doi.org/10.1007/s00248-011-9995-4>, 2012.

422 Gussone, G.: *Supplementum ad Florae Siculae Prodrumum*, Edit. Tramater, Neapoli, 314 pp., 1832.

423 Gandhi, M., Parthiban, S., Thummalu, N. and Christy, A.: NDVI: Vegetation change detection using remote sensing and GIS
424 - A case study of Vellore District, *Procedia Computing Science* 57, 1199–1210, <https://doi.org/10.1016/j.procs.2015.07.415>,
425 2015.

426 Guyette, R. P., Muzika, R .M. and Dey, D. C.: Dynamics of an anthropogenic fire regime, *Ecosystems* 5(5), 472–486,
427 <https://doi.org/10.1007/s10021-002-0115-7>, 2002.

428 Harris, R. M., Remenyi, T. A., Williamson, G. J., Bindoff, N. L., and Bowman, D. M.: Climate–vegetation–fire interactions
429 and feedbacks: trivial detail or major barrier to projecting the future of the Earth system?. *Wiley Interdisciplinary Reviews:*
430 *Climate Change*, 7(6), 910–931, <https://doi.org/10.1002/wcc.428>, 2016.

431 Hijmans, R. J., Cameron, S. E., Parra, J. L., Jone, P. G. and Jarvis, A.: Very high resolution interpolated climate surfaces for
432 global land areas, *International Journal of Climatology* 25, 1965–1978, <https://doi.org/10.1002/joc.1276>, 2005.

433 Hoetzel, S., Dupont, L., Schefuß, E., Rommerskirchen, F., and Wefer, S.: The role of fire in Miocene to Pliocene C4 grassland
434 and ecosystem evolution, *Nature Geosciences*, 6, 1027–1030, <https://doi.org/10.1038/ngeo1984>, 2013.

435 Irl, S. D. H., Steinbauer, M. J., Messinger, J., Blume-Werry, G., Palomares-Martínez, Á., Beierkuhnlein, C., and Jentsch, A.:
436 Burned and devoured - Introduced herbivores, fire, and the endemic flora of the high-elevation ecosystem on La Palma, Canary
437 Islands, *Arctic, Antarctic, and Alpine Research*, 46(4), 859–869, <https://doi.org/10.1657/1938-4246-46.4.859>, 2014.

438 IPCC: Sixth Assessment Report. AR6 Climate Change 2021: The physical science basis.
439 <https://www.ipcc.ch/report/ar6/wg1/#Regional> [Accessed 28 November 2022].

440 Jouffroy-Bapicot, I., Pedrotta, T., Debret, M., Field, S., Sulpizio, R., Zanchetta, G., Sabatier, P., Roberts, N., Tinner, W.,
441 Walsh, K., and Vanni re, B.: Olive groves around the lake. A ten-thousand-year history of a Cretan landscape (Greece) reveals
442 the dominant role of humans in making this Mediterranean ecosystem, *Quaternary Science Reviews*, 267, 107072,
443 <https://doi.org/10.1016/j.quascirev.2021.107072>, 2021.

444 Karadimou, E., Tsiripidis, I., Kallimanis, A. S., Raus, T., and Dimopoulos, P.: Functional diversity reveals complex assembly
445 processes on sea-born volcanic islands, *Journal of Vegetation Science*, 26, 501–512, <https://doi.org/10.1111/jvs.12255>, 2015.

446 Keeley, J. E.: Fire intensity, fire severity and burn severity: a brief review and suggested usage. *International Journal of*
447 *Wildland Fire*, 18(1), 116-126, <https://doi.org/10.1071/WF07049>, 2009.

448 Keeley, J. E., and Brennan, T. J.: Fire-driven alien invasion in a fire-adapted ecosystem. *Oecologia*, 169(4), 1043–1052,
449 <https://doi.org/10.1007/s00442-012-2253-8>, 2012.

450 Key, C. H., and Benson N. C.: Landscape assessment (LA) sampling and analysis methods. USDA Forest Service, Rocky
451 Mountain Research Station, General Technical Report RMRS-GTR-164-CD, 2006.

452 Koutsias, N., and Karteris, M.: Classification analyses of vegetation for delineating forest fire fuel complexes in a
453 Mediterranean test site using satellite remote sensing and GIS. *International Journal of Remote Sensing*, 24, 3093–3104,
454 <https://doi.org/10.1080/0143116021000021152>, 2002.

455 Le Hou rou, H. N.: Land degradation in Mediterranean Europe: can agroforestry be a part of the solution? A prospective
456 review, *Agroforestry Systems* 21, 43–61, <https://doi.org/10.1007/BF00704925>, 1993.

457 Lentile, L. B., Holden, Z. A., Smith, A. M. S., Falkowski, M. J., Hudak, A. T., Morgan, P., Lewis, S. A., Gessler, P. E., and
458 Benson, N. C.: Remote sensing techniques to assess active fire characteristics and post-fire effects. *International Journal of*
459 *Wildland Fire*, 15, 319–345, <https://doi.org/10.1071/WF05097>, 2006.

460 Lo Cascio, P., Ponel, P. and Altadonna, G.: Diversity and distribution of beetles in a Mediterranean volcanic archipelago: an
461 updated checklist of the Coleoptera on the Aeolian Islands (Sicily, Italy). *Biodiversity Journal*, 13(3), 531–
462 585, <https://doi.org/10.31396/Biodiv.Jour.2022.13.3.531.585>, 2022.

463 Lojacono, M.: *Le Isole Eolie e la loro vegetazione, con enumerazione delle piante spontanee vascolari*. Palermo, Lorusnaider,
464 147 pp., 1878.

465 Lozano, O. M., Salis, M., Ager, A. A., Arca, B., Alcasena, F. J., Monteiro, A. T., Finney, M. A., Del Giudice, L., Scoccimarro,
466 E., and Spano, D.: Assessing climate change impacts on wild fire exposure in Mediterranean areas, *Risk Analysis*, 37, 1898–
467 1916, <https://doi.org/10.1111/risa.12739>, 2017.

468 Mantero, G., Morresi, D., Marzano, R., Motta, R., Mladenoff, D. J., and Garbarino, M.: The influence of land abandonment
469 on forest disturbance regimes: a global review, *Landscape Ecology* 35, 2723–2744, <https://doi.org/10.1007/s10980-020-01147-w>, 2020.

471 Massa, B., Lo Cascio, P., Ientile, R., Canale, E., and La Mantia, T.: Gli uccelli delle isole circumsiciliane, *Naturalista siciliano*,
472 39(2), 105–373, 2015.

473 M dail, F.: Plant Biogeography and Vegetation Patterns of the Mediterranean Islands, *The Botanical Review*, 88, 63–129,
474 <https://doi.org/10.1007/s12229-021-09245-3>, 2021.

475 Moriondo, M., Good, P., Durao, R., Bindi, M., Giannokopoulos, C., and Core-Real, J.: Potential impact of climate change on
476 fire risk in the Mediterranean area, *Climate Research*, 31, 85–95, <https://doi:10.3354/cr031085>, 2006.

477 Novara, A., Gristina, L., Rühl, J., Pasta, S., D'Angelo, G., La Mantia, T., and Pereira, P.: Grassland fire effect on soil organic
478 carbon reservoirs in semiarid environments, *Solid Earth*, 4(1-5), 1–13, <https://doi.org/10.5194/se-4-1-2013>, 2013.

479 Palá-Paúl, J., Velasco-Negueruela, A., Pérez-Alonso, M.J., and Sanz, J.: Seasonal variation in chemical composition of *Cistus*
480 *albidus* L. from Spain. *Journal of Essential Oil Research*, 17, 19–22, <https://doi.org/10.1080/10412905.2005.9698818>, 2005.

481 Pasta, S., Ardenghi, N. M. G., Badalamenti, E., La Mantia, T., Livreri Console, S. & Parolo, G.: The alien vascular flora of
482 Linosa (Pelagie Islands, Strait of Sicily): update and management proposals, *Willdenowia*, 47(2), 135–144,
483 <https://doi.org/10.3372/wi.47.47205>, 2017

484 Pasta, S., Guarino, R., La Rosa, A., Lo Cascio, P., Chiarucci, A., Médail, F., Pavon, D., Zannini, P., and Fernández-Palacios,
485 J.M., *Tentamen Florae Aeolicae*: comprehensive checklist and biogeographic analysis of the vascular flora of the Aeolian
486 Archipelago (Sicily, Italy), *Mediterranean Botany*, submitted.

487 Pauchard, A., García, R. A., Pena, E., González, C., Cavieres, L. A., and Bustamante, R. O.: Positive feedbacks between plant
488 invasions and fire regimes: *Teline monspessulana* (L.) K. Koch (Fabaceae) in central Chile, *Biological Invasions*, 10(4), 547–
489 553, <https://doi.org/10.1007/s10530-007-9151-8>, 2008.

490 Pausas, J. G.: Response of plant functional types to changes in the fire regime in Mediterranean ecosystems: a simulation
491 approach, *Journal of Vegetation Science*, 10(5), 717–722, <https://doi.org/10.2307/3237086>, 1999.

492 Pausas, J. G.: Simulating Mediterranean landscape pattern and vegetation dynamics under different fire regimes, *Plant*
493 *Ecology*, 187(2), 249–259, <https://doi.org/10.1007/s11258-006-9138-z>, 2006.

494 Pausas J. G. and Keeley, J. E.: A burning story: the role of fire in the history of life, *BioScience* 59(7), 593–601,
495 doi:10.1525/bio.2009.59.7.10, 2009.

496 Pausas, J. G., and Millán, M. M.: Greening and browning in a climate change hotspot: the Mediterranean
497 Basin, *BioScience*, 69(2), 143–151, <https://doi.org/10.1093/biosci/biy157>, 2019.

498 Picotte, J. J., and Robertson, K. M.: Accuracy of remote sensing wildland fire-burned area in southeastern US Coastal plain
499 habitats, *Tall Timbers Fire Ecol. Proc.*, 24, 86–93, 2010.

500 Pignatti, S., Guarino, R., and La Rosa, M.: *Flora d'Italia*, 4 vols. Edagricole, Edizioni Agricole di New Business Media,
501 Bologna.

502 Ponel, P., Lo Cascio, P., and Soldati, F.: A new species of *Catomus* Allard, 1876 (Coleoptera: Tenebrionidae: Helopini) from
503 the Aeolian Archipelago (Sicily, Italy), *Zootaxa*, 4743(2), 295–300, <https://doi.org/10.11646/zootaxa.4743.2.14>, 2020

504 Richter, M.: Vegetationsdynamik auf Stromboli, *Aachener Geographische Arbeiten*, 16, 41–110, 1984.

505 Richter, M., and Lingenhöhl, D.: Landschaftsentwicklung auf den Äolischen Inseln. Betrachtung in verschiedenen Zeitskalen,
506 *Geographische Rundschau*, 54(4), 20–26, 2002.

507 Ripley, B. S., Visser, V., Christin, P.-A., Archibald, S., Martin, T., and Osborne, C.: Fire ecology of C3 and C4 grasses
508 depends on evolutionary history and frequency of burning but not photosynthetic type, *Ecology*, 96(10), 2679–2691,
509 <https://doi.org/10.1890/14-1495.1>, 2015

510 Rittmann, M.: Der Ausbruch des Stromboli am 11. September 1930. *Zeitschrift für Vulkanologie*, 14, 47-77, 1931.

511 Rivas-Martínez, S. Clasificación Bioclimática de la Tierra, 2004,
512 https://webs.ucm.es/info/cif/book/bioc/global_bioclimatics_2.htm. [Accessed 28 November 2022]

513 Rossetti, I., Cogoni, D., Calderisi, G., and Fenu, G.: Short-Term Effects and Vegetation Response after a Megafire in a
514 Mediterranean Area. *Land*, 11(12), 2328, <https://doi.org/10.3390/land11122328>, 2022.

515 Roy, J., and Sonie, L.: Germination and population dynamics of *Cistus* species in relation to fire, *Journal of Applied Ecology*,
516 29(3), 647–655, <https://doi.org/10.2307/2404472>, 1992.

517 Salis, M., Del Giudice, L., Jahdi, R., Alcasena-Urdiroz, F., Scarpa, C., Pellizzaro, G., Bacciu, V., Schirru, M., Ventura, A.,
518 Casula, M., Pedes, F., Canu, A., Duce, P., and Arca, B.: Spatial patterns and intensity of land abandonment drive wildfire
519 hazard and likelihood in Mediterranean agropastoral areas, *Land*, 11(11), 1942, <https://doi.org/10.3390/land11111942>, 2022.

520 Scheiter, S., Higgins, S. I., Osborne, C. P., Bradshaw, C., Lunt, D., Ripley, B. S., Taylor, L. L., and Beerling, D. J.: Fire and
521 fire-adapted vegetation promoted C4 expansion in the late Miocene, *New Phytologist*, 195(3), 653–666,
522 <https://doi.org/10.1111/j.1469-8137.2012.04202.x>, 2012.

523 Scuderi, D., Di Gregorio, R., Toscano, S., Cassaniti, C., and Romano, D.: Germination behaviour of four mediterranean *Cistus*
524 L. species in relation to high temperature, *Ecological Questions*, 12, 171–180, <https://doi.org/10.12775/v10090-010-0011-2>,
525 2010.

526 Soverel, N.O., Perrakis, D. D. B., and Coops, N. C.: Estimating burn severity from Landsat d NBR and Rd NBR indices across
527 western Canada, *Remote Sensing of Environment*, 114, 1896–1909, <https://doi.org/10.1016/j.rse.2010.03.013>, 2010.

528 Trabaud, L.: Postfire plant community dynamics in the Mediterranean Basin, in: *The Role of Fire in Mediterranean-Type*
529 *Ecosystems*, edited by Moreno, J.M. and Oechel, W.C., Springer, New York, NY, 1–15, [https://doi.org/10.1007/978-1-4613-](https://doi.org/10.1007/978-1-4613-8395-6_1)
530 [8395-6_1](https://doi.org/10.1007/978-1-4613-8395-6_1), 1994.

531 Velasco, A. G. V., Probanza, A., Mañero, F. G., Treviño, A. C., Moreno, J. M., and Garcia, J. L.: Effect of fire and retardant
532 on soil microbial activity and functional diversity in a Mediterranean pasture, *Geoderma*, 153(1-2), 186–193,
533 <https://doi.org/10.1016/j.geoderma.2009.08.005>, 2009.

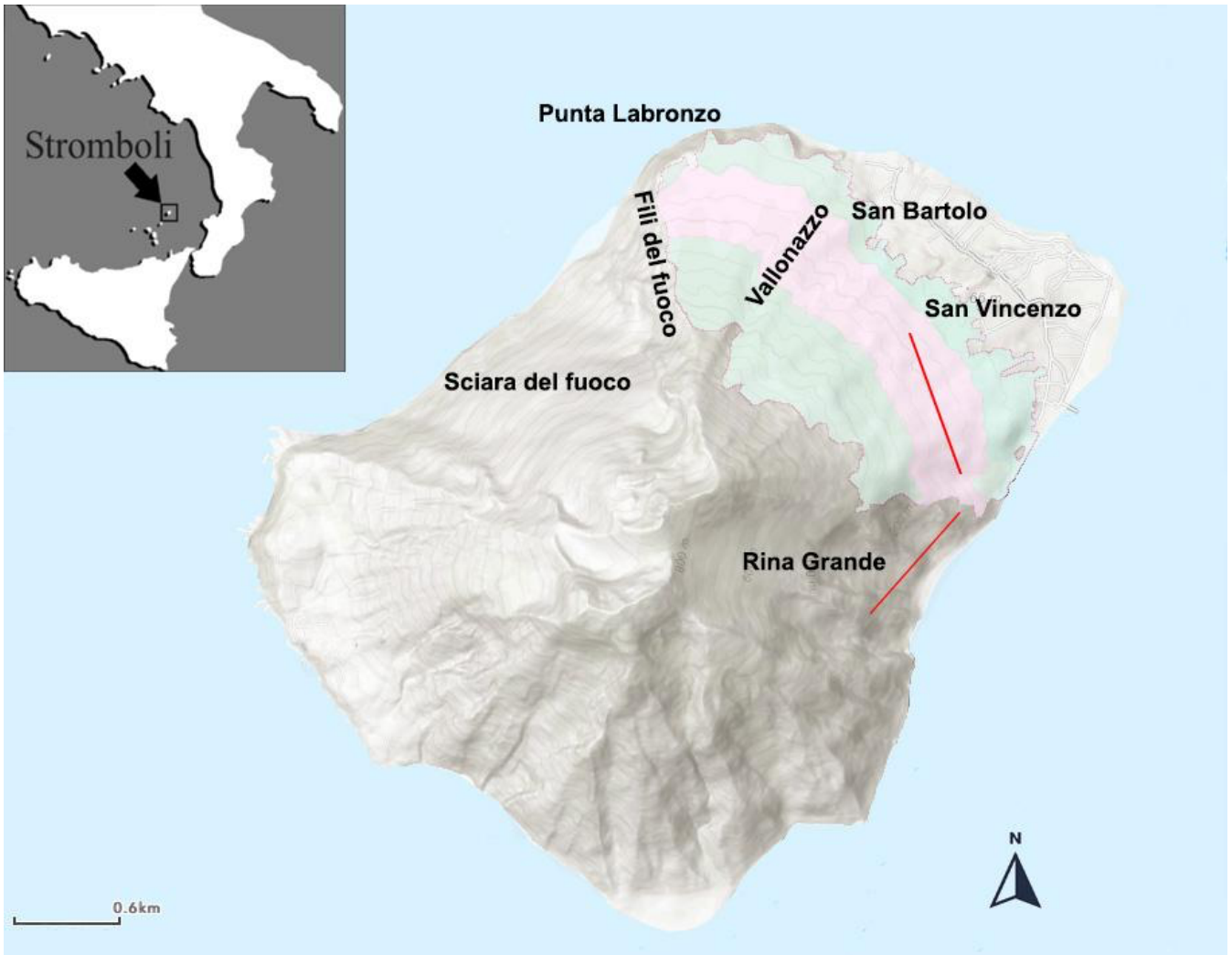
534 Vallejo, V. R., Allen, E. B., Aronson, J., Pausas, J. G., Cortina, J., and Gutiérrez, J. R.: Restoration of Mediterranean-type
535 woodlands and shrublands, in: *Restoration Ecology: The New Frontier*, edited by Andel, J. and Aronson, J. (Eds.), Blackwell
536 Publishing Ltd.: Oxford, UK, 130–144, 2012.

537 Weiser F., Sauer A., Gettueva D., Field R., Irl S.D.H., Vetaas O., Chiarucci A., Hoffmann S., Fernández-Palacios J.M., Otto
538 R., Jentsch, A., Provenzale, A. and Beierkuhnlein, C.: Impacts of forest fire on understory species diversity in Canary pine
539 ecosystems on the island of La Palma. *Forests*, 12(12), 1638, 2021.

540 Zaia, R., Pasta, S., Di Rita, F., Laudicina, V. A., Lo Cascio, P., Magri, D., Troia A., and Guarino, R.: Staying alive on an active
541 volcano: 80 years population dynamics of *Cytisus aeolicus* (*Fabaceae*) from Stromboli (Aeolian Islands, Italy), *Ecological*
542 *Processes*, 9(1), 1–15, <https://doi.org/10.1186/s13717-020-00262-5>, 2020.

543 Hearst, Marti A., et al. "Support vector machines." *IEEE Intelligent Systems and their applications* 13.4 (1998): 18-28.

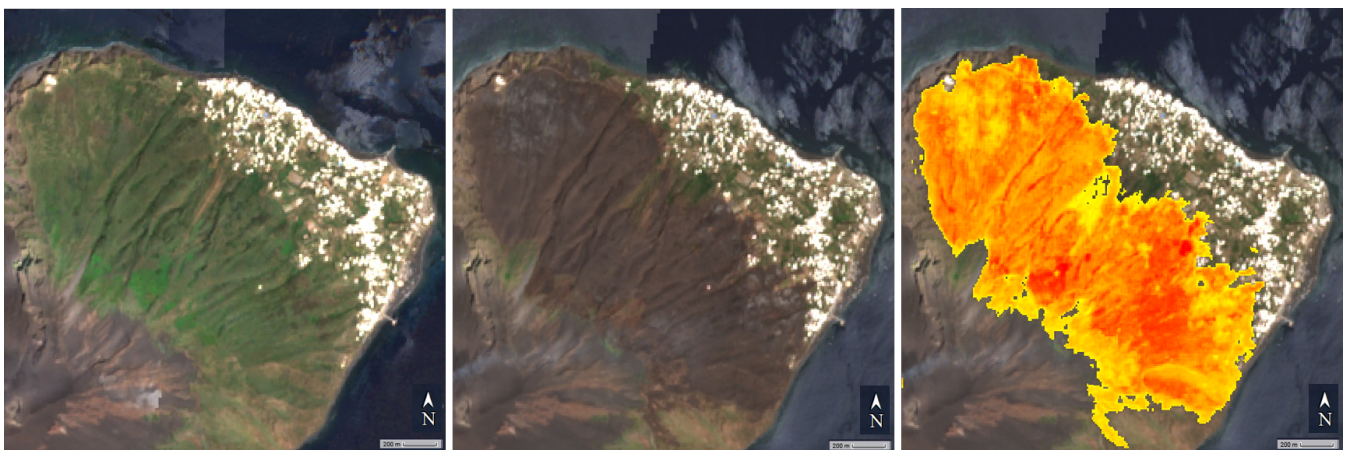
544



545
546
547
548

Figure 1: Map of the study area (light green) with the place names mentioned in the text. The pink colour indicates the area where the vegetation plots for validation were sampled. Red lines identify the two transects along which the stem density of *Saccharum* was measured.

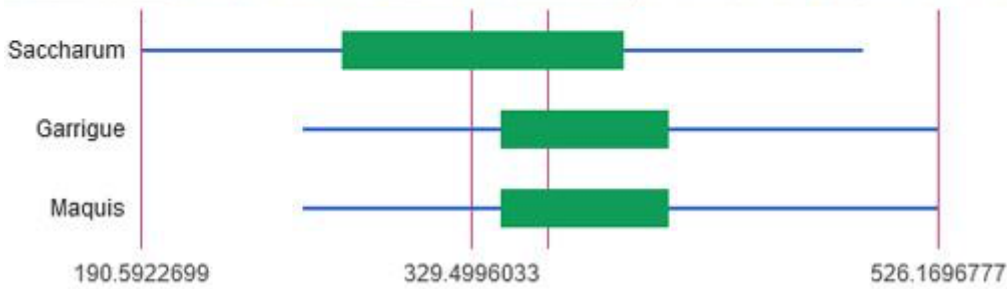
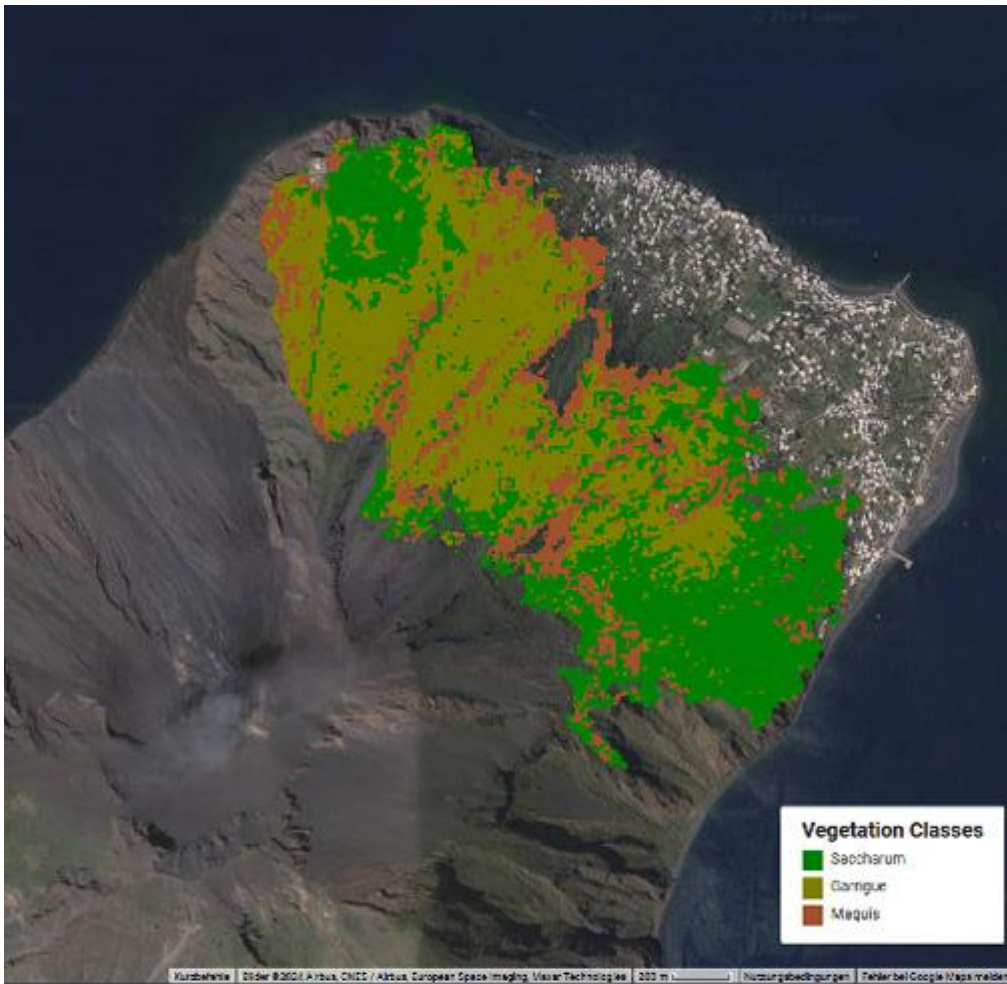
549
550
551



552
553
554
555

Figure 2: (from left to right) Sentinel 2 image before fire event (composite of acquisitions in the time period 22/04 - 22/05/2022); Sentinel 2 image after fire (composite of acquisitions in the time period 25/05/22-15/06/2022); *dNBR*-inferred burned area (yellow: low-, orange: middle-, red: high-severity damage) overlaid on the middle image composite.

556



557

558

559

560

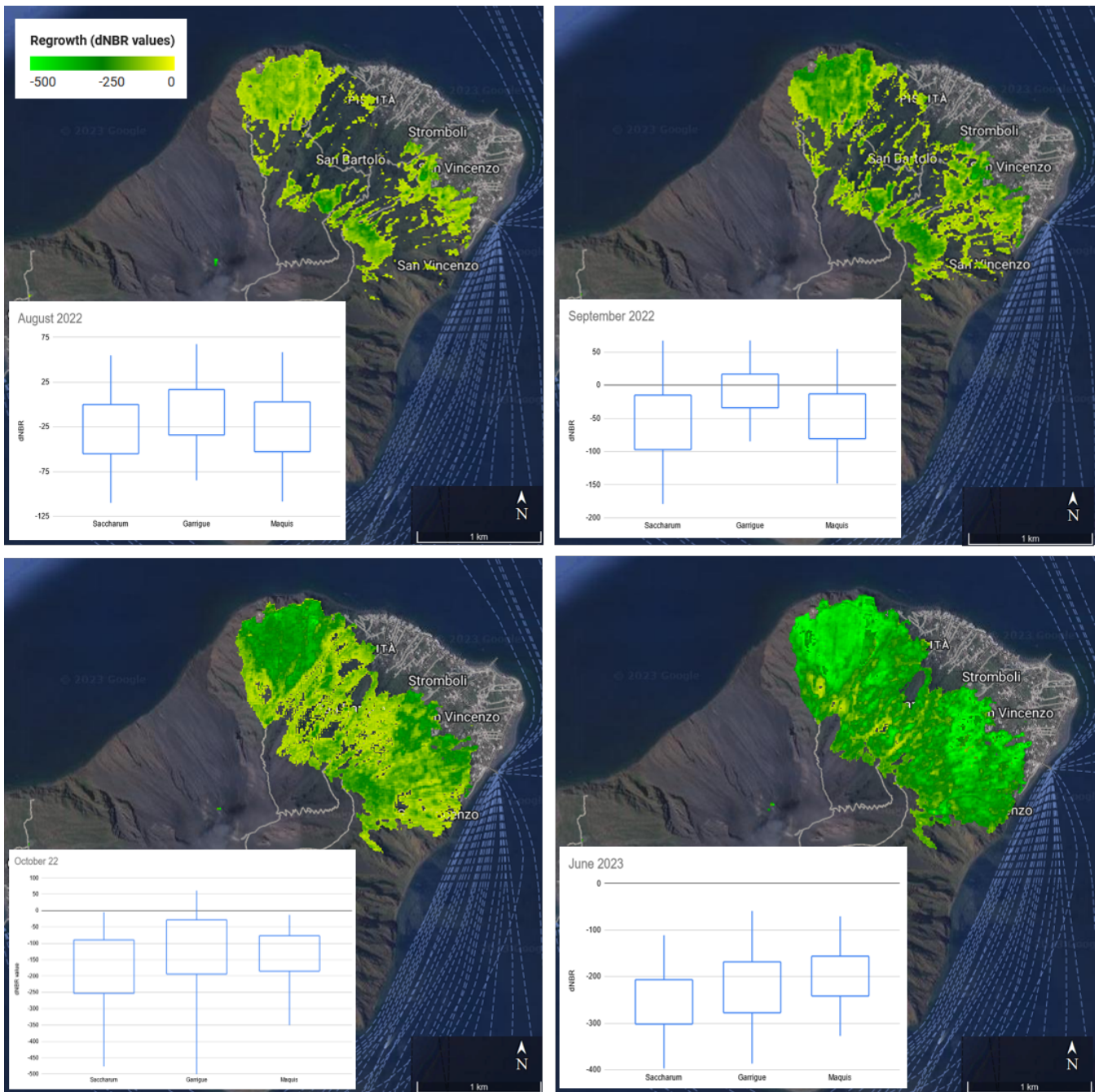
561

562

Figure 3: (top) supervised classification of vegetation classes in the study area, overlaid on Google Earth base map (© 2024 Airbus, CNES/Airbus, European Space Imaging, Maxar Technologies); (bottom) Boxplot showing the distribution of $dNBR$ values per vegetation class, evaluated on the image composites from acquisitions in the periods 15 April - 22 May and 26 May -15 June 2022. Boxes and whiskers correspond to one and two standard deviations, accounting for 68% and 95% of the processed values, respectively. Fire occurred in garrigue and maquis was estimated to be the most severe.

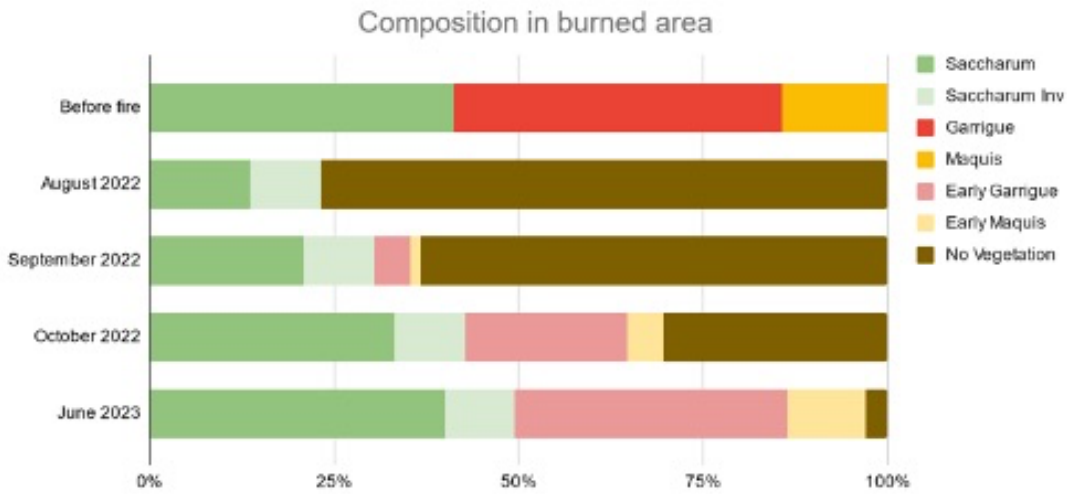


563
564
565
566
567
568
569
570
571
572
Figure 4: (left) high resolution drone image acquired on 17 August 2022 to assess the quality of the information derived from *dNBR* analysis, overlaid on an high resolution image from Google Earth basemap; (top right) pre-fire detail from Google Earth basemap; (middle right) post-fire detail from drone image; (bottom right) same detail with overlaid thresholded *dNBR* values higher than 0.19 (using pre-fire and August 2022 scene), semitransparent for visual comparison (yellow: low-, orange: middle-, red: high- severity damage). Credits of drone images: Antonio Zimbone. Credits for Google base map: © 2024 Airbus, CNES/Airbus, European Space Imaging, Maxar Technologies.



573
 574
 575
 576
 577
 578
 579
 580
 581

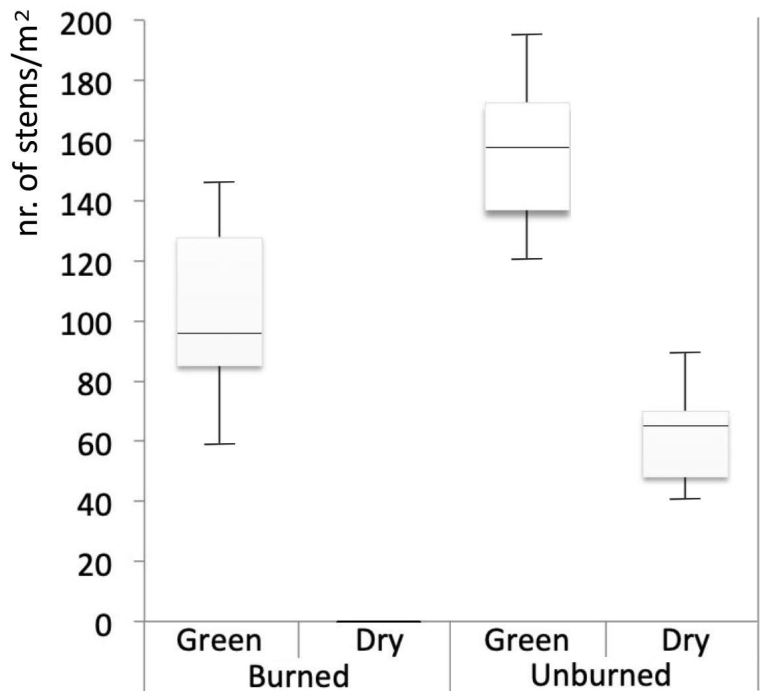
Figure 5: Vegetation recovery in the area affected by the fire, estimated through dNBR values from different acquisitions of Sentinel-2 images, overlaid on Google Earth base map (© 2024 Airbus, CNES/Airbus, European Space Imaging, Maxar Technologies). Boxplots show the distribution of dNBR values associated with recovery in the areas occupied by *Saccharum*, garrigue, and maquis. Boxes and whiskers correspond to one and two standard deviations, accounting for 68% and 95% of the processed values, respectively. The following thresholds were suggested by Key and Benson (1996) to categorise levels of recovery from dNBR values rescaled by 1000: no change from 0 to -100, low enhanced recovery from -100 to -250, and high enhanced recovery (high) from -250. *Saccharum* is characterized by faster recovery than the maquis and the garrigue, particularly at the beginning of the first growing season after fire (September-October 2022).



582
583
584
585
586
587

Figure 6: estimated vegetation composition in the study area (cover %). "Saccharum" vegetation patches occupied by Saccharum both before and after fire; "Saccharum Inv" sums the surface areas previously occupied by other vegetation units and invaded by Saccharum after fire. "Early garrigue" and "Early maquis" refer to early post-fire successional stages of these two vegetation classes, dominated by annual plants, resprouted shrubs and seedlings of perennial seeders, chiefly *Cistus sp. pl.*

588
589



590
591
592

Figure 7: (left) measuring resprouted *Saccharum biflorum* stem density in one of the plots within the burned area (18 Sept. 2022, photo by R. Guarino); (right) boxplots of the stem density of *Saccharum* in burned and unburned patches.



593
594
595

Figure 8: (left) historical photo of terraced vineyards on Stromboli (year: 1891, anonymous), with rows of *Saccharum biflorum* used as windbreaks; (right) same view, 130 years later (16 July 2021, photo by P. Lo Cascio).